Self-Assembly, Characterization, and Chemical Stability of Isocyanide-Bound Molecular Wire Monolayers on Gold and Palladium Surfaces

ARTICLE *in* LANGMUIR · DECEMBER 2005

Impact Factor: 4.46 · DOI: 10.1021/la051094z · Source: PubMed

Self-Assembly, Characterization, and Chemical Stability of Isocyanide-Bound Molecular Wire Monolayers on Gold and Palladium Surfaces

Joshua J. Stapleton,[#] Thomas A. Daniel,[#] Sundarajan Uppili,[#] Orlando M. Cabarcos,[#] Jawad Naciri,[+] Ranganathan Shashidhar,[+,†] and David L. Allara*[,#]

Department of Chemistry and The Materials Research Institute, Pennsylvania State University, University Park, Pennsylvania 16802, and Center for Bio/Molecular Science and Engineering, Naval Research Laboratory, Washington, D.C. 20375

Received April 24, 2005. In Final Form: September 1, 2005

Self-assembled monolayers (SAMs) of the isocyano derivative of 4,4′-di(phenylene-ethynylene)benzene (**1**), a member of the "OPE" family of "molecular wires" of current interest in molecular electronics, have been prepared on smooth, {111} textured films of Au and Pd. For assembly in oxygen-free environments with freshly deposited metal surfaces, infrared reflection spectroscopy (IRS) indicates the molecules assume a tilted structure with average tilt angles of 18−24° from the surface normal. The combination of IRS, X-ray photoelectron spectroscopy, and density functional theory calculations all support a single σ-type bond of the −NC group to the Au surface and a σ/π-type of bond to the Pd surface. Both SAMs show significant chemical instability when exposed to typical ambient conditions. In the case of the Au SAM, even a few hours storage in air results in significant oxidation of the −NC moieties to −NCO (isocyanate) with an accompanying decrease in surface chemical bonding, as evidenced by a significant increase in instability toward dissolution in solvent. In the case of the Pd SAM, similar air exposure does not result in incorporation of oxygen or loss of solvent resistance but rather results in a chemically altered interface which is attributed to polymerization of the −NC moieties to quasi-2D poly(imine) structures. Conductance probe atomic force microscope measurements show the conductance of the degraded Pd SAMs can diminish by ∼2 orders of magnitude, an indication that the SAM−Pd electrical contact has severely degraded. These results underscore the importance of careful control of the assembly procedures for aromatic isocyanide SAMs, particularly for applications in molecular electronics where the molecule−electrode junction is critical to the operational characteristics of the device.

1. Introduction

With the increased interest in fabricating electronic devices based on molecules and molecular assemblies, it is becoming critically important to understand the detailed way in which the molecules bond and organize at electrode surfaces. Self-assembled monolayers (SAMs) have become a useful test bed for investigating the electronic properties of device candidate molecules,[1] as well as being the most common configuration for such devices. One family of candidate structures used extensively in recent studies is based on SAMs made from various derivatives of 4,4′-di(phenylene-ethynylene)benzenethiol[2] [commonly referred to as oligo(phenylene-ethynylene)thiol or OPE-SH]. It has been shown that the current−voltage behavior of these molecules can be altered by changing ring substituents.[3−5] Further flexibility in tailoring the electrical properties of the SAMs is possible by altering the headgroup used to anchor the molecule to the base electrode and by varying the electrode material.[6] While attachment of molecules to a gold substrate via a sulfur atom has been studied extensively,[7,8] far less attention has been paid to alternative attachment chemistries. Of particular note are recent reports showing that bonding to gold via tellurium,[9] selenium,[10−20] and the isocyanide

* To whom correspondence should be addressed. E-mail: David L. Allara: dla3@psu.edu.

[#] Pennsylvania State University.

[+] Naval Research Laboratory.

[†] Present address: Geo-Centers, Inc., Maritime Plaza One, 1201 M Street S. E., Suite 050, Washington, DC 20003.

(1) (a) James, D. K.; Tour, J. M. *Chem. Mater.* **2004**, *16*, 4423−4435. (b) Salomon, A.; Cahen, D.; Lindsay, S.; Tomfohr, J.; Engelkes, V. B.; Frisbie, C. D. *Adv. Mater.* **2003**, *15*, 1881−1890.

(2) Tour, J. M. *Acc. Chem. Res.* **2000**, *33*, 791−804.

(3) Rawlett, A. M.; Hopson, T. J.; Nagahara, L. A.; Tsui, R. K.; Ramachandran, G. K.; Lindsay, S. M. *Appl. Phys. Lett.* **2002**, *81*, 3043−3045.

(4) Chen, J.; Wang, W.; Reed, M. A.; Rawlett, A. M.; Price, D. W.; Tour, J. M. *Appl. Phys. Lett.* **2000**, *77*, 1224−1226.

(5) Chen, J.; Reed, M. A.; Rawlett, A. M.; Tour, J. M. *Science* **1999**, *286*, 1550−1552.

(6) Seminario, J. M.; Zacarias, A. G.; Tour, J. M. *J. Am. Chem. Soc.* **1999**, *121*, 411−416.

(7) Schreiber, F. *Prog. Surf. Sci.* **2000**, *65*, 151−256.

(8) Ulman, A. *Chem. Rev.* **1996**, *96*, 1533−1554.

(9) Nakamura, T.; Yasuda, S.; Miyamae, T.; Nozoye, H.; Kobayashi, N.; Kondoh, H.; Nakai, I.; Ohta, T.; Yoshimura, D.; Matsumoto, M. *J. Am. Chem. Soc.* **2002**, *124*, 12642−12643.

(10) Monnell, J. D.; Stapleton, J. J.; Jackiw, J. J.; Dunbar, T.; Reinerth, W. A.; Dirk, S. M.; Tour, J. M.; Allara, D. L.; Weiss, P. S. *J. Phys. Chem. B* **2004**, *108*, 9834−9841.

(11) Sato, Y.; Mizutani, F. *Phys. Chem. Chem. Phys.* **2004**, *6*, 1328−1331.

(12) Protsailo, L. V.; Fawcett, W. R.; Russell, D.; Meyer, R. L. *Langmuir* **2002**, *18*, 9342−9349.

(13) Patrone, L.; Palacin, S.; Bourgoin, J. P.; Lagoute, J.; Zambelli, T.; Gauthier, S. *Chem. Phys.* **2002**, *281*, 325−332.

(14) Aslam, M.; Bandyopadhyay, K.; Vijayamohanan, K.; Lakshminarayanan, V. *J. Colloid Interface Sci.* **2001**, *234*, 410−417.

(15) Han, S. W.; Kim, K. *J. Colloid Interface Sci.* **2001**, *240*, 492−497.

(16) Bandyopadhyay, K.; Vijayamohanan, K.; Venkataramanan, M.; Pradeep, T. *Langmuir* **1999**, *15*, 5314−5322.

(17) Bandyopadhyay, K.; Vijayamohanan, K. *Langmuir* **1998**, *14*, 625−629.

(18) Huang, F. K.; Horton, R. C.; Myles, D. C.; Garrell, R. L. *Langmuir* **1998**, *14*, 4802−4808.

(19) Dishner, M. H.; Hemminger, J. C.; Feher, F. J. *Langmuir* **1997**, *13*, 4788−4790.

(20) Samant, M. G.; Brown, C. A., Gordon, J. G., II. *Langmuir* **1992**, *8*, 1615−1618.

10.1021/la051094z CCC: $30.25
Published on Web 10/18/2005

group (−N≡C)[21−36] is possible. Furthermore, there has been little work done on the assembly of organic molecules on alternate metals such as palladium, an attractive alternate for device contacts,[21,22,37] despite the fact that electrical measurements of isocyanide SAMs bound on Pd appear to exhibit improved junction properties over those on Au.[38]

Given the reports that −NC/noble metal junctions exhibit lower conduction barriers than the corresponding thiol-based junctions,[29] it is important for molecular electronics applications to establish in detail the attachment mechanism(s) of isocyanide-terminated device-type molecules since the attachment mode could affect the molecular orientation and packing. The differences in charge transport properties between −S and −NC bound molecules are presumably due to variances in the electronic structure of the headgroups which result from different orbital overlaps between the molecular and the electrode surface states. Calculations of a CH_3S- moiety bound to a $(Au)_{16}$ cluster indicate that bonding at a (111) hollow site results in transfer of ∼0.4 e^- to the S atom with residual positive charge on the surrounding gold atoms.[39] The nature of the ArNC−metal bond (where Ar = an aryl group, the common constituent structure of device molecules) is complicated by possible multiple bonding interactions with the metal substrate. For example, in the case of commonly used transition metal electrodes, coordination of ArNC− typically results in a σ-type bond via donation by the carbon lone pair to the metal substrate. When the metal has filled d orbitals capable of overlapping the π^* antibonding orbitals of the −N≡C moiety, a back-donation π-type bond also may form.[40] In the specific case of Au, several reports concluded that the (ArNC)−Au bond is formed dominantly by σ-donation from the carbon lone pair of the isocyanide group to a gold atom (Figure 1, structure I).[21,22,28] In the report of Kubiak and co-workers, it was concluded from a qualitative analysis of their IR data that aromatic isocyanides on Au bond in a vertical manner to the gold surface.[28]

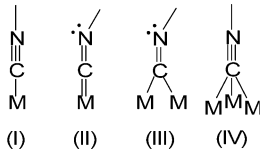

Figure 1. Possible bonding structures for **1**−SAMs on Au (I) and Pd (II, III, or IV).

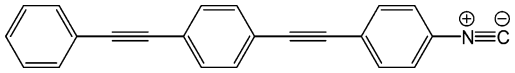

Figure 2. Chemical structure of OPE-NC (**1**).

Two recent studies by Swanson[21] and Bennett[22] utilize infrared (IR) spectroscopy to directly compare the bonding of aromatic isocyanide SAMs on Pd and Au. For adsorption of 1,4-diisocyanobenzene on thermally evaporated Pd films, Bennett et. al. observed a strong IR band at ∼1960 cm^{-1}, considerably lower in frequency than the uncoordinated isocyanide (2127 cm^{-1}), which was interpreted in terms of a back-bonded type of species assigned to either or both of two structures (II and III in Figure 1).[22] In addition, another large band observed at 2170 cm^{-1} was assigned to a σ-donation species (structure I, Figure 1).[41] Time-dependent adsorption studies suggested that the isocyanide group initially bonds through σ donation and eventually shifts to more-stable σ/π sites. Such a result would indicate that the specific morphology of the metal substrate could have a strong effect on the type of bonding. No details of molecular structure such as molecular orientation were given in their paper. In contrast, Swanson et. al. observe only the back-bonded type of coordination for a series of diisocyanide phenylene oligomers adsorbed onto Pd.[21] However, they assign the broad IR band observed in the 1980−2000 cm^{-1} region to a triple-bridging species (structure IV, Figure 1).[21]

In this paper, we present a detailed study of the preparation and characterization of SAMs of the terminal isocyanide derivative of 4,4′-di(phenylene-ethynylene)-benzene (OPE-NC, in Figure 2) on Pd{111} and Au{111} surfaces. Our main interest was to explore in detail the attachment chemistry and SAM molecular structure for the OPE system, used commonly for device measurements, in a closely controlled, parallel study of Au and Pd surfaces, both prepared to have similar surface conditions, and morphologies. Of particular interest was the chemical stability of the molecule−metal bonding under normal preparation and handling conditions since the behavior of a molecular device will depend critically on the integrity of the molecules and their attachment. In general, though there are a number of reports on the electrical characterization of OPE-type SAMs,[3−5,42−59] few details are

(21) Swanson, S. A.; McClain, R.; Lovejoy, K. S.; Alamdari, N. B.; Hamilton, J. S.; Scott, J. C. *Langmuir* **2005**, *21*, 5034−5039.
(22) Murphy, K. L.; Tysoe, W. T.; Bennett, D. W. *Langmuir* **2004**, *20*, 1732−1738.
(23) Caruso, A. N.; Rajesh, R.; Gallup, G.; Redepenning, J.; Dowben, P. A. *J. Phys.-Condens. Mat.* **2004**, *16*, 845−860.
(24) Joo, S. W.; Kim, W. J.; Yun, W. S.; Hwang, S.; Choi, I. S. *Appl. Spectrosc.* **2004**, *58*, 218−223.
(25) Kim, H. S.; Lee, S. J.; Kim, N. H.; Yoon, J. K.; Park, H. K.; Kim, K. *Langmuir* **2003**, *19*, 6701−6710.
(26) Joo, S. W.; Kim, W. J.; Yoon, W. S.; Choi, I. S. *J. Raman Spectrosc.* **2003**, *34*, 271−275.
(27) Bae, S. J.; Lee, C. R.; Choi, I. S.; Hwang, C. S.; Gong, M. S.; Kim, K.; Joo, S. W. *J. Phys. Chem. B* **2002**, *106*, 7076−7080.
(28) Henderson, J. I.; Feng, S.; Bein, T.; Kubiak, C. P. *Langmuir* **2000**, *16*, 6183−6187.
(29) Hong, S.; Reifenberger, R. *Superlattices Microstruct.* **2000**, *28*, 289−303.
(30) Lin, S.; McCarley, R. L. *Langmuir* **1999**, *15*, 151−159.
(31) Huc, V.; Bourgoin, J. P.; Bureau, C.; Valin, F.; Zalczer, G.; Palacin, S. *J. Phys. Chem. B* **1999**, *103*, 10489−10495.
(32) Ontko, A. C.; Angelici, R. J. *Langmuir* **1998**, *14*, 3071−3078.
(33) Ontko, A. C.; Angelici, R. J. *Langmuir* **1998**, *14*, 1684−1691.
(34) Henderson, J. I.; Feng, S.; Ferrence, G. M.; Bein, T.; Kubiak, C. P. *Inorg. Chim. Acta* **1996**, *242*, 115−124.
(35) Shih, K. C.; Angelici, R. J. *Langmuir* **1995**, *11*, 2539−2546.
(36) Robertson, M. J.; Angelici, R. J. *Langmuir* **1994**, *10*, 1488−1492.
(37) Love, J. C.; Wolfe, D. B.; Haasch, R.; Chabinyc, M. L.; Paul, K. E.; Whitesides, G. M.; Nuzzo, R. G. *J. Am. Chem. Soc.* **2003**, *125*, 2597−2609.
(38) Chen, J.; Calvet, L. C.; Reed, M. A.; Carr, D. W.; Grubisha, D. S.; Bennett, D. W. *Chem. Phys. Lett.* **1999**, *313*, 741−748.
(39) Sellers, H.; Ulman, A.; Shnidman, Y.; Eilers, J. E. *J. Am. Chem. Soc.* **1993**, *115*, 9389−9401.
(40) Ugi, I. *Isonitrile Chemistry*; Academic Press: New York, 1974.
(41) Murpy, K.; Azad, S.; Bennett, D. W.; Tysoe, W. T. *Surf. Sci.* **2000**, *467*, 1−9.
(42) Kushmerick, J. G.; Whitaker, C. M.; Pollack, S. K.; Schull, T. L.; Shashidhar, R. *Nanotechnology* **2004**, *15*, S489−S493.
(43) Selzer, Y.; Cabassi, M. A.; Mayer, T. S.; Allara, D. L. *Nanotechnology* **2004**, *15*, S483−S488.
(44) Kushmerick, J. G.; Lazorcik, J.; Patterson, C. H.; Shashidhar, R.; Seferos, D. S.; Bazan, G. C. *Nano Lett.* **2004**, *4*, 639−642.
(45) Fan, F. R. F.; Yao, Y. X.; Cai, L. T.; Cheng, L.; Tour, J. M.; Bard, A. J. *J. Am. Chem. Soc.* **2004**, *126*, 4035−4042.
(46) Fan, F. R. F.; Lai, R. Y.; Cornil, J.; Karzazi, Y.; Bredas, J. L.; Cai, L. T.; Cheng, L.; Yao, Y. X.; Price, D. W.; Dirk, S. M.; Tour, J. M.; Bard, A. J. *J. Am. Chem. Soc.* **2004**, *126*, 2568−2573.
(47) Khondaker, S. I.; Yao, Z.; Cheng, L.; Henderson, J. C.; Yao, Y. X.; Tour, J. M. *Appl. Phys. Lett.* **2004**, *85*, 645−647.
(48) Kushmerick, J. G.; Naciri, J.; Yang, J. C.; Shashidhar, R. *Nano Lett.* **2003**, *3*, 897−900.
(49) Reichert, J.; Ochs, R.; Beckmann, D.; Weber, H. B.; Mayor, M.; von Lohneysen, H. *Phys. Rev. Lett.* **2002**, *88*, 176804.
(50) Kushmerick, J. G.; Holt, D. B.; Yang, J. C.; Naciri, J.; Moore, M. H.; Shashidhar, R. *Phys. Rev. Lett.* **2002**, *89*, 086802.

available on their chemical and structural nature,[60−66] particularly in the case of isocyanide-bound SAMs where only a few studies are available for aromatic-type SAMs,[21,22,28] with only one including an OPE type of molecule.[28] Thus, it is critical that the structural and chemical properties be thoroughly investigated if the electrical behaviors of OPE-NC SAMs are to be interpreted on a fundamental basis.

Our methodology utilizes multiple characterization techniques including quantitative infrared reflection spectroscopy (IRS), X-ray photoelectron spectroscopy (XPS), single wavelength ellipsometry (SWE), atomic force microscopy (AFM) in both tapping and conducting probe (CP-AFM) modes, liquid drop contact angles, and quantum chemical calculations (primarily to assist in vibrational mode assignments). With these techniques, we have been able to probe a variety of SAM characteristics ranging from molecular orientation to the molecule−substrate bonding. The results confirm the presence of a single, σ-type −NC/Au surface bond but show, in contrast to the earlier results, that only a σ/π-type bond forms on Pd when smooth, {111} textured surfaces are used. Furthermore, both SAMs show very similar molecular orientation with ∼24° tilt angles of the long molecular axis. Most importantly, with implications for molecular devices, the present study shows that even brief exposures to an ambient environment for minutes to hours can result in significant degradation of the attachment bonding of both SAMs. In the case of Au, the degradation consists of oxidation of isocyanide to isocyanate with complete loss of chemical bonding, consequent disordering of the film, and loss of solvent resistance. In the case of Pd, exposure results in a cross-linking reaction of the −NC groups to a quasi-2D imine polymer, again with loss of chemical bonding. In both cases, these effects will result in significant loss in the junction integrity of a molecular device. This prediction is confirmed directly by conducting probe atomic force microscope measurements for the Pd case.

2. Experimental Section

2.1. Synthesis. Details of the synthesis and characterization of OPE-isocyanide (compound **1**, Figure 2) are given in the Supporting Information.

2.2. Sample Preparation. The metal films were deposited onto silicon substrates (∼1.5 nm of native oxide) which were cleaned with H_2O_2/H_2SO_4 solution,[63] rinsed copiously with water and ethanol, and then blown dry with N_2. In the case of the Au films, ∼5 nm of Cr was first deposited from a heated rod coated with Cr followed by ∼200 nm of Au deposited from a resistive boat (background pressure $<3 \times 10^{-8}$ Torr during all depositions). The Pd depositions were carried out using argon ion sputtering (saddle field ion guns obtained from South Bay Tech, Torrance, CA) of the metal targets and sequential deposition of ∼5 nm Cr and ∼175 nm Pd films onto a rotating substrate. The Au/Cr/SiO_2/Si and Pd/Cr/SiO_2/Si films typically showed rms roughness of 1.2(±0.2) and 0.8(±0.15) nm, respectively, by tapping mode AFM. Gold films prepared in this way have been shown previously to be highly {111} textured,[67] while X-ray diffraction analysis of the Pd films (using the CHESS facility at Cornell) showed a highly {111} textured surface with the grains oriented 3(±9)° from the surface normal.[68] The freshly evaporated metal substrates were immediately characterized by SWE and then used within 15 min ambient exposure to form the SAM.

Monolayer preparation was carried out in a nitrogen-purged glovebox with the O_2 concentration kept below 2 ppm to avoid oxidative degradation of the reagents and the SAMs. All solutions were mixed and stored in screwtop fluoroware containers. SAMs of OPE-NC were formed in 1 mM solutions prepared by dissolving the compound in dichloromethane (freshly distilled over P_2O_5 under a nitrogen atmosphere). The substrates then were added, and the solution stored overnight (∼18−24 h). After monolayer formation, the wafers were rinsed with distilled dichloromethane and dried under a stream of N_2. Prior to removal from the glovebox and to minimize ambient exposure, the samples were sealed in nitrogen-filled bags for transfer to the various measurement tools.

2.3. Characterization Methods. The SWE measurements were recorded at 632.8 nm using a Stokes ellipsometer (Gaertner Scientific Corporation, LSE Stokes Ellipsometer, Skokie, IL) set at a 70° angle of incidence. The experimental polarization angles were used to determine film thickness using well-established modeling methods.[69,70] For simplicity, the thickness was based on isotropic film models in which the complex refractive index is described as a scalar, $\hat{n} = n + ik$. More-rigorous anisotropic models were not considered since accurate values for the elements of the diagonalized refractive index tensor are not available and the variations from the isotropic model were assumed to be close to the error limits of our measurements (∼±0.1 nm). The absorption index (k) (at 632.8 nm) was set to zero, while n was estimated from atom-fragment quantitative structure−activity relationships (QSAR)[72] to give a value of 1.73. The required mass density was obtained using the atom-fragment density estimation method. This method has predicted mass densities within 5% of the known values for similar compounds.[67]

The reflection IR spectra were collected using a custom, in-house-modified spectrometer (DigiLab, FTS-7000, Randolph, MA) as described in detail elsewhere.[74] The spectrometer and external

(51) Kushmerick, J. G.; Holt, D. B.; Pollack, S. K.; Ratner, M. A.; Yang, J. C.; Schull, T. L.; Naciri, J.; Moore, M. H.; Shashidhar, R. *J. Am. Chem. Soc.* **2002**, *124*, 10654−10655.
(52) Fan, F. R. F.; Yang, J. P.; Cai, L. T.; Price, D. W.; Dirk, S. M.; Kosynkin, D. V.; Yao, Y. X.; Rawlett, A. M.; Tour, J. M.; Bard, A. J. *J. Am. Chem. Soc.* **2002**, *124*, 5550−5560.
(53) Amlani, I.; Rawlett, A. M.; Nagahara, L. A.; Tsui, R. K. *Appl. Phys. Lett.* **2002**, *80*, 2761−2763.
(54) Donhauser, Z. J.; Mantooth, B. A.; Kelly, K. F.; Bumm, L. A.; Monnell, J. D.; Stapleton, J. J.; Price, D. W.; Rawlett, A. M.; Allara, D. L.; Tour, J. M.; Weiss, P. S. *Science* **2001**, *292*, 2303−2307.
(55) Reed, M. A.; Chen, J.; Rawlett, A. M.; Price, D. W.; Tour, J. M. *Appl. Phys. Lett.* **2001**, *78*, 3735−3737.
(56) Creager, S.; Yu, C. J.; Bamdad, C.; O'Connor, S.; MacLean, T.; Lam, E.; Chong, Y.; Olsen, G. T.; Luo, J. Y.; Gozin, M.; Kayyem, J. F. *J. Am. Chem. Soc.* **1999**, *121*, 1059−1064.
(57) Cygan, M. T.; Dunbar, T. D.; Arnold, J. J.; Bumm, L. A.; Shedlock, N. F.; Burgin, T. P.; Jones, L.; Allara, D. L.; Tour, J. M.; Weiss, P. S. *J. Am. Chem. Soc.* **1998**, *120*, 2721−2732.
(58) Dhirani, A.; Lin, P. H.; GuyotSionnest, P.; Zehner, R. W.; Sita, L. R. *J. Chem. Phys.* **1997**, *106*, 5249−5253.
(59) Bumm, L. A.; Arnold, J. J.; Cygan, M. T.; Dunbar, T. D.; Burgin, T. P.; Jones, L.; Allara, D. L.; Tour, J. M.; Weiss, P. S. *Science* **1996**, *271*, 1705−1707.
(60) Richter, L. J.; Yang, C. S. C.; Wilson, P. T.; Hacker, C. A.; Stapleton, J. J.; Allara, D. L.; Yao, Y.; Tour, J. M. *J. Phys. Chem. B* **2004**, *108*, 12547−12559.
(61) Hacker, C. A.; Batteas, J. D.; Garno, J. C.; Marquez, M.; Richter, C. A.; Richter, L. J.; van Zee, R. D.; Zangmeister, C. D. *Langmuir* **2004**, *20*, 6195−6205.
(62) Walzer, K.; Marx, E.; Greenham, N. C.; Less, R. J.; Raithby, P. R.; Stokbro, K. *J. Am. Chem. Soc* **2004**, *126*, 1229−1234.
(63) Stapleton, J. J.; Harder, P.; Daniel, T. A.; Reinard, M. D.; Yao, Y. X.; Price, D. W.; Tour, J. M.; Allara, D. L. *Langmuir* **2003**, *19*, 8245−8255.
(64) Yang, G. H.; Qian, Y. L.; Engtrakul, C.; Sita, L. R.; Liu, G. Y. *J. Phys. Chem. B.* **2000**, *104*, 9059−9062.
(65) Zehner, R. W.; Sita, L. R. *Langmuir* **1997**, *13*, 2973−2979.
(66) Dhirani, A. A.; Zehner, R. W.; Hsung, R. P.; GuyotSionnest, P.; Sita, L. R. *J. Am. Chem. Soc* **1996**, *118*, 3319−3320.
(67) Dunbar, T. D.; Cygan, M. T.; Bumm, L. A.; McCarty, G. S.; Burgin, T. P.; Reinerth, W. A.; Jones, L.; Jackiw, J. J.; Tour, J. M.; Weiss, P. S.; Allara, D. L. *J. Phys. Chem. B.* **2000**, *104*, 4880−4893.
(68) Daniel, T. A.; Smilgies, D.; Allara, D. L. unpublished results.
(69) Collins, R. W.; Kim, Y. T. *Anal. Chem.* **1990**, *62*, 887−890.
(70) Shi, J.; Hong, B.; Parikh, A. N.; Collins, R. W.; Allara, D. L. *Chem. Phys. Lett.* **1995**, *246*, 90−94.
(71) Parikh, A. N.; Allara, D. L. Effects of Optical Anisotropy on Spectro-Ellipsometric Data for Thin Films and Surfaces. In *Optical Studies on Real Surfaces and Inhomogeneous Thin Films*; Francombe, M., Ed.; Physics of Thin Films Series; Academic Press, New York, 1994; Vol. 19, pp 279−323.
(72) Ghose, A. K.; Crippen, G. M. *J. Chem. Inf. Comput. Sci.* **1987**, *27*, 21−35.
(73) Immirzi, A.; Perini, B. *Acta. Crystallogr.* **1977**, *A33*, 216−218.
(74) Parikh, A. N.; Allara, D. L. *J. Chem. Phys.* **1992**, *96*, 927−945.

optics were purged with nitrogen gas. All spectra were taken at an 86° angle of incidence with p-polarized light and the instrument resolution set to 2 cm^{-1}. Reflection spectral intensities are reported as $-\log(R/R_0)$, where R is the power reflectivity of the IR beam and R_0 is the reflectivity of a reference sample. Several different reference samples were used depending on the spectral region of interest and included $C_{16}D_{32}S$/Au or Pd SAMS, $C_{18}H_{36}S$/Au or Pd SAMS, and wafers of freshly evaporated gold and palladium films. Note that the decreased signal-to-noise in the spectra of the **1**−Pd SAM compared to **1**−Au SAM is due to the lower reflectivity of palladium in the mid-IR.[75]

The XPS analyses were performed on a monochromatic Al Kα source instrument (Kratos, Axis Ultra, England). Spectra were collected with a photoelectron takeoff angle of 90° and a 40 eV pass energy. All spectra were reference to the C 1s binding energy at 285.0 eV.

Dynamic advancing and receding contact angles were measured using a home-built video-interfaced apparatus. All measurements were made with the sample exposed to ambient. A 20 μL drop of Milli-Q water (Millipore Products, Bedford, MA) was dispensed onto the surface using a flat-tipped micrometer syringe (GS-1200, Gilmont Instruments, Barrington, IL). The advancing contact angle was measured as the drop expanded. The drop was then partially retracted into the syringe, and the receding angle measured. Images of the drop were captured digitally using a CCD camera, and contact angles were analyzed using ImageJ 1.32j software (National Institutes of Health, USA). The typical time required to obtain an advancing and receding contact angle is less than 5 min. Measurements were made on at least three separate spots for each sample.

Tapping mode AFM images were taken using a Dimension Series 3100 (Digital Instruments, Santa Barbara, CA) scanning probe microscope using 125-μm-long etched silicon tips (Nanosensors, NCH type, Neuchatel, Switzerland) with typical resonant frequencies between 270 and 330 kHz. The conducting probe measurements (CP-AFM) were performed in a UHV chamber (base pressure 10^{-10} Torr) outfitted with a RHK 350 sample probe setup controlled by a RHK SPM 100 electronics system (RHK technologies, Troy, MI). Electrical measurements were made with double-side Pt−Ir-coated cantilevers with EFM-type tips (spring constant ≈ 2.8 N/m, tip radius ≈ 20 nm; Molecular Imaging, Tempe, AZ). Current−voltage (I−V) measurements were made for each SAM as follows. First, tip damage was minimized by careful sample approach. Once surface contact was established, force−distance measurements were used to verify the tip integrity and any damaged tips were discarded. During I−V measurements, the applied force on the tip was kept as low as possible, generally settling around 10 nN due to the limitations of the attractive forces. The measurements were then performed by sweeping the surface bias over ±1 V.

3. Results and Discussion

3.1. Molecular Structure of SAMs Prepared in Oxygen-Free Conditions. *3.1.1. Film Thickness.* The average monolayer thicknesses determined using SWE are 2.1(±0.1) and 1.9(±0.1) nm, respectively, for SAMs of **1**−Au and **1**−Pd. In comparison, the physical length of the molecule, as determined from the optimized geometry in our DFT calculations (see Supporting Information), is 2.17 nm from the terminal hydrogen to the isocyanide carbon. While this comparison appears to suggest that the molecules are arranged with the long axis oriented exactly perpendicular to the surface, we note that no attempt was made to account for the possibility of an optically distinct carbon−metal interface in our modeling of the data, and this may contribute to small errors in the deduced film thickness.[70,76] Given the experimental errors and the uncertainty of the interfacial optical properties, the SAM film thicknesses cannot be readily interpreted in more detail in terms of the differences between the two SAMs and the inferred molecule orientation.

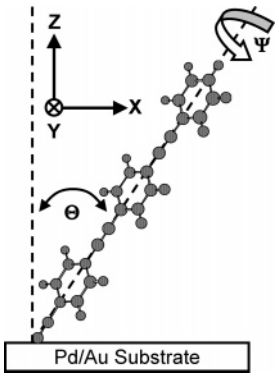

Figure 3. Definition of the tilt (θ) and twist (Ψ) angles of an OPE molecule relative to the laboratory coordinate system, where the laboratory coordinate, *Z*, is perpendicular to the sample surface. When the molecule is aligned with the long molecular axis parallel to *Z* and the aromatic rings in the *XZ* plane, the *xyz* molecular coordinate system is aligned with the laboratory *XYZ* system.

3.1.2. Film Surface Character: Surface Wetting and AFM. Advancing (θ_{adv}) and receding (θ_{rec}) water contact angles of 72(±2)° and 51(±2)°, respectively, were obtained for the **1**−Au SAM and 87(±2)° and 67(±2)° for the **1**−Pd SAM, respectively, with a common hysteresis [$\theta_{adv} - \theta_{rec}$] of ∼20°. In comparison, θ_{adv}, θ_{rec} and hysteresis values of 78°, 69°, and 9°, respectively, were reported for the analogous OPE-thiolate SAM on Au.[63] The relatively higher hysteresis for the isocyanide SAMs on Au and Pd compared to the thiolate SAM on Au suggests the presence of a lower packing density and additional surface defects in the isocyanide SAMs.[77] Repeated measurements at different spots on the same sample over a span of roughly 15−20 min in an ambient environment showed no obvious changes in the contact angle values over time, an indication that the contact angle values are intrinsic to the freshly made samples.[78]

The average rms surface roughness values, measured by tapping mode AFM of the bare Au and Pd substrates are 1.2(±0.2) and 0.8(±0.2) nm, respectively, and those of the **1**−Au−SAMs and the **1**−Pd−SAMs are 1.1(±0.1) and 0.7(±0.1) nm, respectively. These data show that the SAMs are highly conformal, on average, to the substrates.[79]

3.1.3. Molecular Orientation. Quantitative reflection IR spectroscopy was used to determine the average molecular tilt (θ) and twist (ψ) angles of the molecules in the SAMs, where the angles are defined in Figure 3.

The IR spectral analyses used are briefly summarized for reference. For details, see the previously published work.[63] The vibrational modes utilized in the orientation analysis are listed in Table 1 along with their spectral notations, based on Wilson−Varsanyi terminology,[80] and the assigned transition dipole directions.

(75) For example, see: Greenler, R. G. *J. Vac. Sci. Tech.* **1975**, *12*, 1410−1417.

(76) Spectroscopic ellipsometric measurements would be required to identify a distinct optical interfacial layer and measure the thickness and complex optical function characteristics (see ref 70).

(77) Bain, C. D.; Troughton, E. B.; Tao, Y. T.; Evall, J.; Whitesides, G. M.; Nuzzo, R. G. *J. Am. Chem. Soc.* **1989**, *111*, 321−335.

(78) A number of cyclic voltammetry measurements for the different SAMs under different conditions were run to further probe the packing density of the SAMs. In all cases, the CVs showed almost no current-blocking capability for the SAMs and changed with each successive sweep, approaching the bare electrode behavior over time, an indication that the measurement conditions degraded the SAM.

(79) A number of attempts were made to obtain evidence for molecular ordering in the case of the **1**−SAM on Au{111} on mica substrates. Using methods previously successful in obtaining images of ordered molecules for the OPE thiolate SAM on Au{111} (see ref 63), no evidence for ordering in the **1**−Au SAM could be obtained.

Table 1. IR Mode Assignments for Polycrystalline 1 and the 1−Au SAM

mode[a]	frequency, cm^{-1} bulk	frequency, cm^{-1} SAM	transition dipole direction[b]	I_{exp}[c]	I_{exp}/I_{iso}[d]
C≡C stretch	2210	2212	*z*	0.84	3.65
N≡C stretch	2125	2190	–	–	–
(8a)	1596	1596	*z*	0.43	3.07
(19a)[f]	1515	1517	*z*	2.90	1.27
(19a)[f]	1509	1505	*z*	1.26	1.22
(19a)[f]	1483	1485	*z*	0.80	1.91
(18b) r_3	1104	*e*	*x*	0.02	0.03
(18b) r_1	1070	1069	*x*	0.08	0.38
(18a) r_1	1027	1026	*z*	0.45	3.75
(18b) r_2, r_3	1016	1017	*z*	0.42	1.36
aryl C−H op r_3, r_2	846, 840	837[g]	*y*	0.44	0.10
aryl C−H op r_1	762	755	*y*	0.64	0.32
aryl C−H op r_1	694	689	*y*	0.46	0.35

[a] Mode descriptions are in terms of Wilson's terminology for aromatic rings. r_1 is the top monosubstituted phenyl ring, r_2 is the middle ring, and r_3 is the isocyanide-substituted ring. op = out of the plane of the phenyl ring. For details see text. [b] Transition Dipole Direction. *z* is parallel to the long molecular axis, *x* is perpendicular to the *z* axis in the plane of the phenyl rings, and *y* is perpendicular to the ring plane. The directions were estimated by analysis of DFT theory calculations. For details see text. [c] I_{exp} is the intensity in the experimental SAM spectrum in absorbance units multiplied by a scaling factor of 10^3. [d] I_{iso} is the intensity in the simulated spectra of a 2.10 nm thick isotropic film of **1** multiplied by a scaling factor of 10^3. [e] No peak was detected; the intensity of the mode was approximated as an upper limit by the noise level. [f] Three separate modes with 19a character were identified in which each mode had vibrational motion involving all three aromatic rings. [g] Due to signal-to-noise limitations in the OPE-NC SAM spectra, the peak centered at 837 cm^{-1} was not resolved into the individual components observed in the bulk spectra. For the orientation analysis, the area under this peak was treated as a single mode since the transition dipole direction is the same for each mode.

All peak assignments were based on literature assignments of analogous molecules[81] combined with our DFT calculations of the isolated molecule (see Supporting Information for details of the calculated isolated molecule vibrational spectrum). The direction of each transition dipole moment vector was assigned from the DFT-determined nuclear Cartesian displacement vector of the mode and then represented in terms of the projections along the directions of the long molecular axis (*z*) and the in- and out-of-plane directions relative to the central aromatic ring (*x* and *y*, respectively; see Table 1). A simulated isotropic monolayer spectrum was generated from transmission spectra of the pure compound dispersed in KBr (see Supporting Information for details). The simulated vibrational mode intensities were then used to normalize the intensity of the experimental reflection spectra. These modes were grouped into *x*, *y*, and *z* subsets, and the ratios of the diagnostic peak areas used in conjunction with the intrinsic transition dipole directions to determine the average orientation using previously described methods.[63] The analysis yields an average molecular tilt and twist of $\theta = 24(\pm 13)°$ and $\psi = 48(\pm 14)°$, respectively, for the case of the **1**−Au SAM. These results support the qualitative conclusion of Kubiak and coworkers of a vertical orientation to the substrate surface for aromatic isocyanides.[28] In our analysis, the N≡C stretch was excluded due to perturbation of the mode upon adsorption on the Au surface. Note the shift of this mode from 2125 cm^{-1} (molecule in KBr dispersion) to 2180−2190 cm^{-1} (SAM), consistent with an aromatic isocyanide bonding to a gold surface (structure I, Figure 1).[28] The orientation analysis was verified by a simulation of the monolayer spectra using thickness and orientation values of 1.85 nm and $\theta = 24°$, $\psi = 48°$, respectively. The experimental and simulated spectra of the **1**−Au SAM are shown in Figure 4.

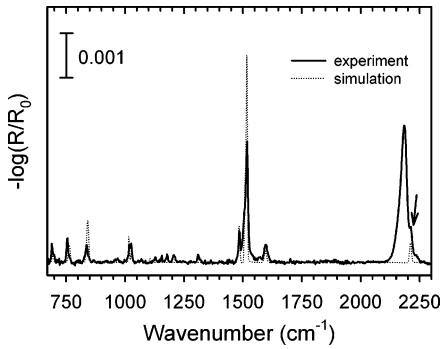

Figure 4. IR spectra of the **1**−Au SAM: experiment (—), simulated spectrum (···). At the high-frequency side of the strong N≡C stretching peak (2190 cm^{-1}), an arrow indicates the position of the C≡C stretching mode peak (~2210 cm^{-1}), present as a shoulder in the experimental spectrum and as a dotted peak in the simulation. The simulation was based on an anisotropic optical tensor derived from transmission spectra of the bulk polycrystalline state of the molecule with a model incorporating a 1.85 nm SAM thickness and an average molecular tilt and twist of 24° and 48°, respectively. The N≡C mode was not included in the simulation since it is perturbed by surface bonding.

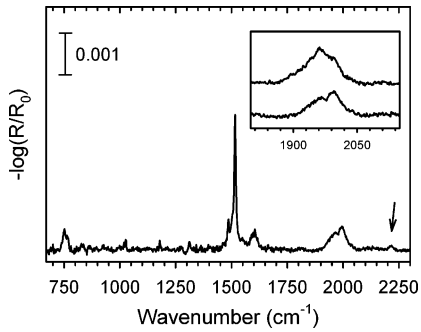

Figure 5. IR spectra of the **1**−Pd SAM. The inset shows the variation typically observed for the NC stretching region. The arrow indicates the position of the weak C≡C stretching mode feature (~2210 cm^{-1}).

The IRS spectrum for **1**−Pd SAM is shown in Figure 5. Average molecular tilt and twist angles of $\theta = 18(\pm 11)°$ and $\psi = 56(\pm 11)°$, respectively, were estimated using the intensity ratio method. These values are the same as for the **1**−Au SAM within experimental error. Note, however, that we consider these values less reliable than the corresponding **1**−Au SAM values for two reasons. First, the *x*-direction modes are close to the noise level in the spectra (note that the spectra are weaker for Pd than Au due to intrinsic differences in the metal reflectivities). Second, the stronger substrate−molecule bonding, presumed to be present in the Pd case compared to Au, likely will cause some degree of perturbation in the electronic structure of the molecule with corresponding effects on some of the vibrational modes and their transition dipole moments (see below). The vibrational modes utilized in the orientation analysis of **1**−Pd SAM are given in the Supporting Information.

3.1.4. Headgroup−Substrate Bonding. The IRS spectra show clear evidence for differences in the −NC/substrate bonding for the two SAMs. In general, while the spectra

(80) Varsanyi, G. *Assignments for Vibrational Spectra of Seven Hundred Benzene Derivatives*; John Wiley and Sons: New York, 1974.
(81) Socrates, G. *Infrared and Raman Characteristic Group Frequencies*; John Wiley and Sons, Ltd: Chichester, 2001.

are similar overall, there are two important differences that can be interpreted in terms of the substrate bonding. First, in the case of Au, note the +65 cm^{-1} shift in the N≡C stretching frequency in moving from the polycrystalline molecule to the **1**−Au SAM (Table 1), an indication of N≡C bond strengthening upon complexation. In contrast, the **1**−Pd SAM spectrum shows the N≡C stretch at ∼1970 cm^{-1}, a corresponding shift of −155 cm^{-1} from the polycrystalline molecule and an indication of N≡C bond weakening upon Pd complexation. This result is consistent with earlier reports of a feature in the ∼1960−2000 cm^{-1} region for various phenylene diisocyanide molecules adsorbed on thermally evaporated Pd film surfaces.[21,22] Overall, the IRS results support a change from a dominantly single-bond substrate attachment for Au (structure I, Figure 1) to dominantly multiple-bonded σ/π coordination for Pd (2-fold, bridged or triple-bridging; structures II, III, or IV).[82] It is important to note that in contrast to the observation of a strong feature at 2170 cm^{-1} by Bennett and co-workers, assigned by them to a σ-donation species, we never observe a feature at frequencies higher than ∼1970 cm^{-1}. We speculate that this difference could arise from different morphologies of the Pd surfaces in the studies.[83] Thus, in our study with smooth [0.8 (±0.2) nm rms roughness], highly {111} textured metal surfaces, only evidence for the σ/π bonding mode is observed.

Second, note the presence of a clear shoulder at ∼2210 cm^{-1}, assigned to the C≡C stretching mode, in the **1**−Au SAM, whereas the corresponding C≡C stretching feature in the **1**−Pd SAM spectrum is noticeably weaker. Further, the simulated and observed **1**−Au SAM spectra (Figure 4) shows comparable C≡C stretching intensities. Given the similar molecular orientations in the SAMs on Au and Pd (see above), explanations of the intensity differences of the C≡C stretching mode cannot be on the basis of orientation. The most likely explanation is in terms of differences in the intrinsic transition dipole moment of the C≡C stretch that arise from shifts in the local charge symmetry around the C≡C group with changes in surface bonding. In particular, the 2-fold coordinations (structures II, III) with Pd should strongly diminish the −NC bond order while the simple single-bond coordination of the Au SAM (structure I) actually appears to improve the −NC bonding. In turn, any reduction in −NC bond order will reduce the isocyanide dipole moment, in turn reducing the C≡C charge asymmetry and, thus, the IR transition intensity.[84]

In support of the conclusions from the IR spectra, the XPS N 1s core level spectra (Figures 6a and 7a) reveal different substrate bonding for the two SAMs.[85] In the case of the Au SAM, the peak is centered at 400.1 eV, in good agreement with a previous report for an aromatic isocyanide bound to gold.[31] In the Pd case, the peak is shifted 1.6 eV lower to 398.5 eV, indicating a greater negative charge on the nitrogen. This corresponds well with the bonding scheme implied from the IR data in which the order of the N≡C bond is reduced for Pd as compared to Au. Overall, from the IRS and XPS data, it does not appear possible for the case of Pd to distinguish between the specific structures represented by the limits of structures II, III, and IV. In a preliminary exploration of the relative energetics of these structures, we have carried out DFT calculations, starting at the very simple level of one and two metal atoms with an isolated molecule, which suggest a preference for structure III over structure II in the case of the **1**−Pd SAM. (see Supporting Information).

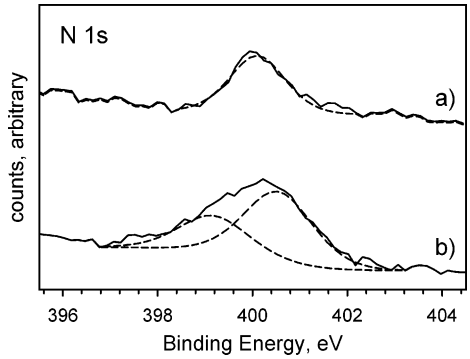

Figure 6. XPS N 1s region spectra: (a) fresh **1**−Au SAM, (b) **1**−Au SAM after 4 h of exposure to laboratory atmosphere. Spectra were collected with a photoelectron takeoff angle of 90° and a pass energy of 40 eV.

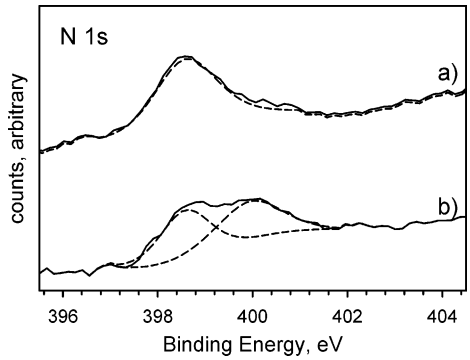

Figure 7. XPS N 1s region spectra: (a) fresh **1**−Pd SAM, (b) **1**−Pd SAM after 4 h of exposure to laboratory atmosphere. Spectra were collected with a photoelectron takeoff angle of 90° and a pass energy of 40 eV.

3.2. Chemical Composition and Stability. *3.2.1. Conversion of Isocyanide to Isocyanate Groups during Ambient Exposure of **1**−Au SAMs.* The −N≡C stretching mode spectrum of a freshly made **1**−Au SAM, prepared in an inert atmosphere glovebox and immediately placed in a N_2-purged IR chamber, is shown in Figure 8. After even only a 60 s additional exposure to ambient, a new

(82) In more detail, note that the broad ∼1970 cm^{-1} peak can be readily fit as contributions from two peaks at ∼1965 and ∼1995 cm^{-1} (see inset of Figure 4). This observation suggests bonding perturbations from different types of Pd surface sites, consistent with the inhomogenity of the textured {111} surface.

(83) Bennett and co-workers report that their Pd films were deposited to ∼10−20 nm thicknesses and were "amorphous with many imperfections" and appeared as "puddles" in SEM images.[21] One might expect that such rough surfaces with a variety of defect sites (kinks, high-energy faces, etc.) might lead to bonding sites with different molecule−metal interactions, including pure σ-bonding sites, and variations in the corresponding vibrational modes. As a check on this possibility, a set of Pd films were made in the same way as our standard films except with the deposition carried out by e-beam deposition at ∼10^{-5} Torr. This procedure resulted in ∼2 nm rms surface roughness (tapping mode AFM), ∼2.5 times the roughness of our standard films (∼0.8 nm rms). Given that the IRS spectrum for the corresponding OPE-NC SAM on this rougher substrate shows no evidence for a feature in the vicinity of 2170 cm^{-1}, we conclude that, if surface morphology were a factor in the appearance of this peak, much rougher films, or equivalently a much larger fraction of high energy substrate defects, would be needed.

(84) A comparison of the IRS spectra for **1**−Au SAM in this work with previously reported work on thiolate-bound OPE−Au SAMs (see ref 63) is instructive in showing the effects of the terminal moiety on the C≡C mode intensity. First, experimentally we observe k(OPE-NC)/k(OPE−SH) ∼5:1, where k is the imaginary (loss) part of the dielectric function for the C≡C stretching mode peak in the pure polycrystalline solids. Consistent with this, our quantum chemical calculations for the isolated molecules show a corresponding ratio of ∼10:1. Finally, for the two SAMs on Au, both bound to the substrate by single bonds, the C≡C stretching peak is clearly observable for the OPE-NC but in the noise for the thiol analogue. Since the thickness and tilt angles of the two SAMs are quite similar, we conclude that the stronger intensity of the −NC SAM on Au is due to intrinsic effects of the headgroup.

(85) C 1s spectra also were taken but showed no significant differences between the two SAMs as expected.

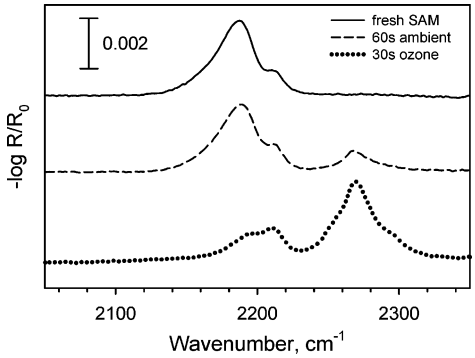

Figure 8. IR spectra of the **1**−Au SAM after different exposures: fresh SAM (—); SAM exposed to ambient laboratory atmosphere for 60 s (- - -); SAM exposed to a concentrated O_3 atmosphere for 30 s (·····).

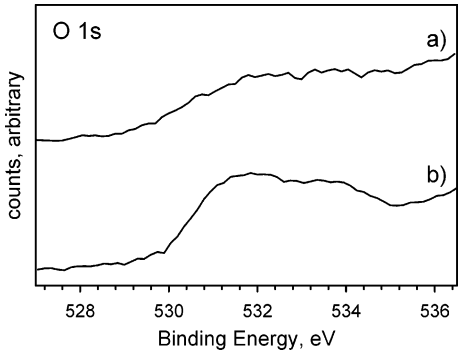

Figure 9. XPS O 1s region spectra: (a) fresh **1**−Au SAM, (b) **1**−Au SAM after 4 h of exposure to laboratory atmosphere. Spectra were collected with a photoelectron takeoff angle of 90° and a pass energy of 40 eV.

peak appears at ~2270 cm^{-1} which can be assigned to an isocyanate (−N=C=O) stretching mode.[81] The fact that the appearance of the new peak is concomitant with a decrease in the intensity of the 2190 cm^{-1} −N≡C stretching mode peak suggests that the new peak arises at the expense of some of the original −N≡C groups. Further, monolayers exposed to ambient for a period of even a few minutes become susceptible to partial removal of the molecules by solvent rinsing, as seen by SWE and IRS (data not shown). Control experiments with exposure to either pure nitrogen or pure oxygen atmospheres or exposure to standard room light under pure nitrogen resulted in negligible changes to the IR spectra, solvent stability, and SWE measurement. In contrast, exposure to an O_3 atmosphere in the dark, prepared by running an UV−ozone cleaning chamber with subsequent insertion of the sample after the UV lamp was turned off,[86] resulted in severe changes, even for brief times (see Figure 8). This behavior is consistent with a previous report of the efficient conversion of isocyanide compounds to isocyantes by ozone.[87] This comparison suggests that in the ambient atmosphere of our laboratory traces of O_3 are present in sufficient amounts[88] to rapidly cause the following reaction of the **1**−Au SAM:

$$R{-}N{\equiv}C{-}(Au) + O_3 \rightarrow R{-}N{=}C{=}O(Au) + O_2$$

This is a significant observation since typical laboratory environments may contain sufficient traces of ozone[88] to be deleterious to the integrity of the isocyanide SAMs.

Finally, consistent with the formation of isocyanate groups, the ozone-degraded SAM has very poor solvent stability, as evidenced by SWE and IRS measurements (data not shown), whereas a freshly made **1**−Au SAM is stable to solvent washing. The ability to wash off a majority of the molecules from the ozone-exposed SAM is consistent with the formation of isocyanate groups since these would be expected to have negligible affinity to chemisorb at a Au surface and would be attached only via weak physisorption forces.

This behavior is analogous to the report of oxidation of alkanethiolate-bound monolayers on silver and gold by traces of O_3 in laboratory environments from which the ozone can penetrate through defects in the SAM to the substrate interface to convert thiolate to sulfinates and sulfonates.[89] In the case of the current **1**−Au SAM, the packing of the monolayer appears to be somewhat less dense and organized than for alkanethiolate SAMs and thus should be at least or more susceptible to penetration and induced degradation by small oxygen species such as O_2 and O_3.

The N1s and O 1s XPS spectra further establish the chemical composition of fresh and degraded monolayers. Deconvolution of the N 1s spectrum of the ozone-oxidized SAM (Figure 6b) yields peaks at 400.5 and 399.2 eV. The higher binding energy peak is in good agreement with the peak observed for a fresh SAM (Figure 6a), while the additional peak shifted to a lower binding energy is consistent with the conversion of an isocyanide to an isocyanate. The fresh SAM does show an O 1s feature, which we attribute to contamination. The growth of the feature in the oxidized SAM, however, is consistent with formation of isocyanate (Figure 9a, b).[90] We note that the oxidative degradation of several diisocyanide SAMs has been reported recently.[21] In contrast to the oxidation of surface-bound monoisocyanide moieties reported in our experiments, the authors of the diisocyanide SAM study[21] interpret IR spectra of their SAMs in terms of only the terminal, unbound isocyanide groups undergoing oxidative degradation.[91]

*3.2.2. Conversion of Isocyanide Groups to Poly(imine) Units during Ambient Exposure of **1**−Pd SAMs.* Upon

(86) Qualitative O_3 exposure experiments were conducted in a commercial UV−ozone cleaner (UVOCS, T10X10/0ES, Montgomeryville, PA). The ozone cleaner was turned on for 10 min with the exhaust vent disabled to facilitate the accumulation of O_3. The UV lamp was then turned off, and the sample introduced into the box for the desired amount of time.

(87) Feuer, H.; Rubinstein, H.; Nielsen, A. T. *J. Org. Chem.* **1958**, *23*, 1107−1109.

(88) The air quality monitoring station maintained by the Pennsylvania Department of Environmental Protection in State College, PA reported that while these experiments were conducted the daily maximum ozone levels were ~50 ppb (www.dep.state.pa.us/aq_apps/ozone/summary.htm). This atmospheric concentration of ozone likely does not reflect the localized concentration of ozone in our laboratory, which is likely effected by the presence of certain equipment such as an ozone cleaner. No attempt was made to quantify the concentration of ozone in our laboratory.

(89) Schoenfisch, M. H.; Pemberton, J. E. *J. Am. Chem. Soc.* **1998**, *120*, 4502−4513.

(90) In principle, analysis of the O 1s spectra should provide a measure of the fraction of isocyanide groups converted to isocyanate, but the quantification of the O 1s region is complicated by several factors. First, the spectrum for the fresh SAM unexpectedly shows a weak O 1s peak. This contamination is likely a combination of adsorbed water and other oxidized material from the ambient onto the gold substrate. Second, XPS of a bare gold wafer exposed to the ambient for a short time shows an analogous O 1s feature. It is possible that the weak NC−Au bond formed during self-assembly is incapable of displacing small amounts of contamination on the gold surface. To check this possibility, XPS spectra were taken over the O 1s region for $CH_3(CH_2)_{15}NC{-}Au$ and $CH_3(CH_2)_{15}S{-}Au$ SAMs. The alkyl isocyanide SAM exhibited a peak similar to that in Figure 9a, while the alkanethiolate film showed no oxygen contamination. We attribute this observation to the aggressive nature of the S−Au bond which we typically observe is conducive to displacing small amounts of contamination. The marked increase in oxygen content for **1**−Au SAMs exposed to the ambient (Figure 9b), however, is consistent with the isocyanide group undergoing oxidation.

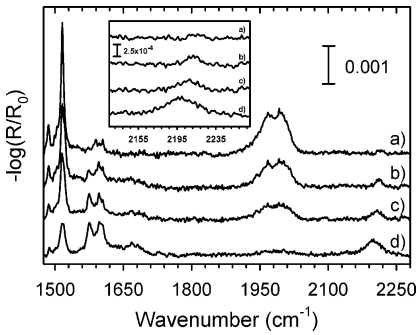

Figure 10. IRS spectra for **1**−Pd SAM after exposure to the laboratory ambient for 0, 4, 24, and 72 h are shown in a, b, c, and d, respectively. The inset shows the high-frequency spectra with a magnified absorbance scale.

exposure of the **1**−Pd SAM to the laboratory ambient, our IRS data show N≡C stretching mode changes that indicate a change in the NC/Pd bonding modes and the appearance of new peaks which indicates the formation of poly(iminomethylene) (−N=C<) from the polymerization of isocyanide groups. The IRS spectra for the **1**−Pd SAM after exposure to the laboratory ambient for 0, 4, 24, and 72 h are shown in spectra a, b, c, and d of Figure 10, respectively. Over the total exposure time, the SWE film thickness remains constant within error (±0.1 nm),[92] an indication that the molecular coverage is constant and variations in the IR spectra are due to chemical changes. The 1970 cm^{-1} peak intensity decay reveals a loss of the (−NC)−Pd substrate bonding modes upon exposure to the ambient. The parallel appearance of peaks in the 1570−1670 cm^{-1} region is consistent with the formation of −N=C< poly(imine) species.[30,95−97] In agreement, repeated rinsing of degraded **1**−Pd films results in only a minimal loss of material (as measured by SWE), consistent with the formation of insoluble polymeric species. The changes observed in the higher-frequency region (see inset of Figure 10) indicate that upon ambient exposure some fraction of the SAM molecules adopt a structure which possess increased charge asymmetry around the C≡C group. This is evidenced by the appearance of the C≡C stretching peak at ∼2210 cm^{-1} after ∼4 h of ambient exposure. This peak position is analogous to the C≡C stretch of the **1**−Au SAM which derives its intensity from the linear −NC/substrate bonding configuration (see Section 3.1.4). In the 4 h degradation spectra-, the lack of an N≡C stretch at ∼2190 cm^{-1} negates the possibility of linearly bound −NC byproducts. These species however, may be present in samples exposed to the ambient for longer periods, viz. a broad peak centered about 2198 cm^{-1} is evident in the spectra of the **1**−Pd SAM after 72 h of exposure. The extent of conversion of the initial −NC groups under our ambient conditions can be estimated from the IR spectra. Presuming that all of the loss of the NC groups is due to polymerization, integration of the 1900−2050 cm^{-1} region features in Figure 10, a measure of the remaining NC groups, indicates that 35, 57, and 89% of the starting SAM is converted to polymer at ∼4, 24, and 72 h, respectively.

The XPS data support these conclusions. The N 1s binding energy for a polyisocyanide-type nitrogen species has been reported as ∼398.5 eV.[31,93] Due to the overlap of the polyisocyanide and palladium-bound isocyanide N 1s species, XPS could not be used to independently establish the presence of a polymeric species on the surface. However, upon exposure to the ambient, a broadening of the 398.5 eV peak is observed. We attribute this to the presence of both polymerized isocyanide [poly(imine)] species and isocyanides bound to the palladium with 2-fold or bridged coordination. Additionally, upon exposure to the ambient, a new peak grows in at ∼400 eV (Figure 7b). While the appearance of this peak is concomitant with SAM degradation, we have not definitively assigned the related surface species.[94] Interference from the strong Pd 3p peak complicates quantitative analysis of the O 1s region for **1**−Pd SAMs, but a qualitative analysis indicates no obvious change upon exposure to the ambient. This is interpreted as meaning that if any oxygen species are present the amounts are negligible.

Ours is not the first report of poly(iminomethylene) (equivalently, polyisocyanide) formation from isocyanide-bound SAMs. Palacin[31] et. al. have shown that 1,4,-phenylene diisocyanide SAMs contain polymer contamination after self-assembly, while McCarley[30] et. al. used IRS to show that upon ambient storage SAMs of 1,6-diisocyanohexane formed polyisocyanides. The use of transition metal catalysts for the polymerization of isocyanides is a well-known route to producing polyisocyanides.[95−98] More relevant to this work is the fact that palladium-containing catalysts have been used to initiate this polymerization,[95−97] and in certain systems, the yields increase when the reaction is run under air rather than N_2.[98] The exact mechanism of the **1**−Pd SAM reaction remains uncertain with respect to the specific effect of oxygen species.[99]

(91) Our data suggest that the complex changes in the diisocyanide spectra may result from oxidation of both isocyanide groups, though likely each isocyanide group on a molecule would react at different rates.

(92) Any effects degradation may have on the SAM/Pd interface were not accounted for in our SWE model.

(93) Brant, P. *J. Electron. Spectrosc. Relat. Phenom.* **1984**, *33*, 153−162.

(94) The growth of a peak at ∼400 eV indicates the presence of a nitrogen species with diminished electron density as compared to isocyanides bound to palladium with 2-fold or bridged coordination. The species responsible for this peak may also account for the appearance of features in the IRS spectra (∼2180−2220 cm^{-1}) which we attribute to a structure possessing increased charge asymmetry around the C≡C group. A few such species possessing greater positive charges on their nitrogen atoms are isocyanates (−N=C=O), linearly bound isocyanides (see structure I, Figure 1) and other possible polymerization products. While IR spectra of the >24 h degraded **1**−Pd SAM indicate that a very small percentage of molecules may adopt the linear binding scheme, this would account for only a small fraction of the area observed under the 400 eV peak. Additionally, the IR spectra reveal a continual change in the nature of the SAM as exposure increases from 4 to 72 h while the XPS N 1s core level spectra remain strikingly similar and possess a static area ratio of ∼ 2:1 for the 398.5/400 eV species. As seen in the XPS N 1s core level spectra of the degraded **1**−Au SAMs, the peak corresponding to an isocyanate species appears at ∼399 eV, ∼1 eV lower in energy than the peak we observe in this case. Also it is unlikely that the isocyanate species are present in the degraded **1**−Pd SAMs given the absence of the strong NCO stretch at ∼2270 cm^{-1} in the IRS. Finally, the structure

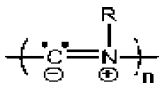

has been proposed as one possible structure for the homopolymerization of isocyanides. This structure was speculative in nature, and Millich et al. had no data to support its existence in their work [see: Millich, F. *Chem. Rev.* **1972**, *2*, 101−113.]. However, this less thermodynamically favored structure has been found for polyacetonitrile, and it exhibits an IR absorption at about 1580 cm^{-1} [see: Millich, F.; Sinclair, R. G. *J. Polym. Sci., Part C* **1968**, *22*, 33−43.]. The possibility of this structure as a byproduct of the **1**−Pd SAM degradation cannot be ruled out given our data, i.e., IRS (appearance of 1575 and 2210 cm^{-1} bands) and XPS (growth of peak at ∼400 eV).

(95) Hida, N.; Takei, F.; Onitsuka, K.; Shiga, K.; Asaoka, S.; Iyoda, T.; Takahashi, S. *Angew. Chem., Int. Ed.* **2003**, *42*, 4349−4352.

(96) Takei, F.; Yanai, K.; Onitsuka, K.; Takahashi, S. *Chem. Eur. J.* **2000**, *6*, 983−993.

(97) Onitsuka, K.; Yanai, K.; Takei, F.; Joh, T.; Takahashi, S. *Organometallics* **1994**, *13*, 3862−3867.

(98) Deming, T. J.; Novak, B. M. *J. Am. Chem. Soc.* **1993**, *115*, 9101−9111.

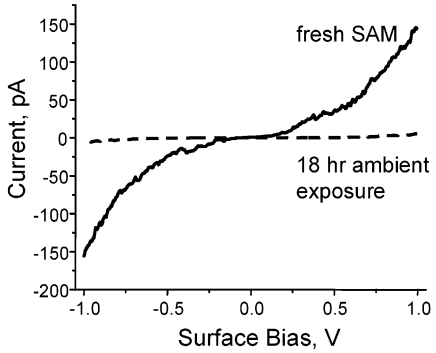

Figure 11. CP-AFM I−V scans for a representative **1**−Pd SAM before and after 18 h of ambient exposure. The curves represent an average of 186 and 240 measurements for the fresh and exposed SAM, respectively, with respective standard deviations of ±60 and ±8 pA. For details, see the text.

*3.2.3. Conductance (CP-AFM) Measurements on the Chemically Degraded **1**−Pd SAM.* It is clear that exposure of the **1**−Au SAM to ambient, or especially active [O], environments causes disruption of the chemical contact of the molecules to the Au substrate via formation of isocyanate groups with accompanying disordering of the SAM and loss of stability toward dissolution in solvents. In this case, the electrical integrity of the molecule−gold contact obviously would be severely degraded by ambient exposure. On the other hand, since the degradation of the **1**−Pd SAM does not cause noticeable loss of solvent stability, independent CP-AFM I−V measurements were made to measure the electrical contact properties directly and assess any loss of conduction at the molecule−Pd junction.

The measurements were made by introducing the sample into the measurement chamber (base pressure, 1×10^{-10} Torr) through a loadlock system, selecting a specific cantilever from a set of available ones stored in the vacuum chamber and then performing sets of ±1 V sweeps. To obtain good statistics, a set of four consecutive scans was made with the selected tip at a given surface location. The tip was then moved to another location to repeat the scan set such that at least 12 arbitrarily chosen different locations on the surface were sampled. The I−V data were then averaged for each tip giving at least 48 data points. In addition, complete sets of I−V measurements were performed using three different tips. This protocol was followed for different **1**−Pd SAMs in which each SAM was sampled when freshly made and again after ambient exposure for 18 h. Representative results, shown in Figure 11, are based on three tips scanning a total of 62 different spots (standard deviation of ±60 pA at 1 V bias) for the unexposed sample and three tips scanning a total of 80 different spots (standard deviation of ±8 pA at 1 V bias) after 18 h of ambient exposure.[100]

The results clearly show on average a severe decrease of the SAM−Pd junction conductance, by ~2 orders of magnitude, after 18 h of exposure to ambient. The much larger fluctuations in the measurements for the exposed sample (±60 vs ±8 pA) are due primarily to spot-to-spot variations across the sample surface. Given the approximate tip−molecule contact area of ~10 nm^2 (an ~20 nm radius of tip curvature applied with ~10 nN force), contact involves <100 molecules. This result suggests that the integrity of the molecule−Pd contact varies roughly over this distance scale, or greater, across the ambient exposed SAM surface. Further, from the integration of the 1900−2050 cm^{-1} region of IR data in Figure 10, we estimate that roughly 50% of SAM is converted to polymer (see Section 3.2.2) in ~18 h. Thus it would appear that the distribution of the polymerized fractional area is in regions at the rough scale of tens of nanometers or smaller.

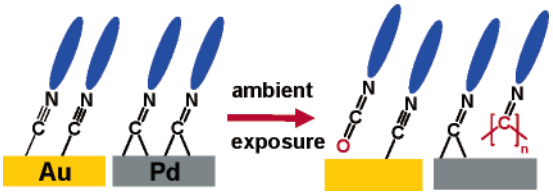

Figure 12. Schematic illustration of the main chemical and structural features of the SAMs on Au and Pd substrates prepared under rigorous conditions with minimum exposure to laboratory ambient and after storage in laboratory ambient. The SAM-on-Au illustration (left) shows the tilted molecule orientation with a single donor−acceptor bond between the −N≡C group and a Au substrate in the case of the freshly made SAM and the subsequent formation of a weakly physisorbed isocyanate group after exposure to ambient conditions with oxygen species present. The SAM-on-Pd illustration, in contrast, shows the same type of tilted molecule structure but with an initial bridge-bonded isocyanide group which slowly converts to a polymeric species over time at ambient temperature. In the case of the Pd SAM, the headgroups, while stable to oxidation reactions, slowly convert with time to a poly(imine) type of polymer film with associated loss in organization and packing of the molecules.

4. Summary and Conclusions

The results are summarized with reference to the schematic illustrations in Figure 12, which show SAM molecule−substrate bonding structures with linear and bridged Au and Pd surface bonds, respectively. Our conclusions are in agreement with previous studies that have proposed these types of structures,[22,28] including a possible 3-bonded structure of the **1**−Pd SAM,[21] but conflict with the earlier proposal of an additional σ/Pd bonding mode.[22] We attribute this latter discrepancy to differences in substrate character such as morphology and conclude that on smooth, highly {111} textured Pd surfaces only the σ/Pd bonding mode forms. Further work to resolve this issue would require UHV studies involving single crystals.

In general, the SAMs are highly conformal to the substrates, as shown by AFM roughness measurements, and the IRS data reveal an average tilt angle of the long molecular axis of ~24° away from the surface normal and a twist angle of ~48° of the aromatic ring plane around

(99) Some of the complications are illustrated by the following observations. When the **1**−Pd degrades during ambient exposure, an isocyanate peak is not observed in the IR spectrum. Upon exposure of the SAM to ozone for 2 min, a very small isocyanate stretching mode peak is observed, in contrast to the observation of the very large intensity of this peak with only a few seconds exposure of a **1**−Au SAM. Further, the remainder of the IRS peaks for the ozone-exposed **1**−Pd monolayer appears similar to Pd SAM samples exposed to the ambient; for example, the 1970 cm^{-1} peak vanishes, the C≡C stretching mode appears with some broadening to indicate appearance of a second, lower energy vibration, and similar peaks appear in the 1570−1670 cm^{-1} region.

(100) No direct CP-AFM data on OPE SAMs appears to be available for comparison with our I−V curves, but two studies have been done with SAMs of the three phenyl ring molecule [1,1′:4′,4″-terphenyl]-4-thiol on gold. Frisbie and co-workers applied ±0.3 V sweeps and report a 130 pA current at a 0.3 V tip bias [Wold, D. J.; Haag, R.; Rampi, M. A.; Frisbie, C. D. *J. Phys. Chem. B* **2002**, *106*, 2813]. Ishida and co−workers in a similar study report ~1 nA currents at a 1 V tip bias [Takao Ishida, T.; Mizutani, W.; Liang, T.-T.; Azehara, H.; Miyake, K.; Sasaki, S.; Tokumoto, H. *Ann. N. Y. Acad. Sci.* **2003**, *1006*, 164−186]. Considering the variations that one would expect from typical variations in tip−molecule contact areas and from the intrinsic differences between the molecule−Au and −Pd junctions, these data compare reasonably with our observation of ~100−150 pA at a 1 V tip bias for the OPE-NC/Pd SAM.

the long molecular axis for both SAMs. Most significantly, preparation and/or storage of the SAMs under ambient laboratory conditions can produce further reactions of the isocyanide headgroups to form new species which degrade the organization and alter the properties of the SAM.

In the case of the SAM on Au, exposure to a laboratory environment, which typically contains traces of active oxygen species such as ozone or singlet oxygen, e.g., as provided by electrical equipment and/or visible and UV radiation, can lead to loss of chemical bonding to the substrate via oxidation of isocyanide to isocyanate groups, with resultant losses in important SAM characteristics including molecular organization and solvent stability. In the case of the SAM on Pd, while exposure to ambient conditions does not appear to cause incorporation of oxygen in the SAM, loss of chemical bonding to the substrate can occur via polymerization of the isocyanide to poly(imine). In this case, while substrate debonding does occur, solvent resistance of the SAM remains, presumably due to the polymeric character of the degraded regions of the SAM. The debonding observed for the SAMs suggests that the electrical integrity of SAM molecule−electrode substrate contacts would be severely degraded. This is confirmed for the case of the degraded **1**−Pd SAM, where electrical contact might be expected to be maintained better than for Au since polymerization should hold the molecules in place adjacent to the electrode surface. Extensive CP-AFM measurements, in fact, show that the electrical conductance of ambient exposed **1**−Pd SAMs can be reduced by roughly 2 orders of magnitude, even for only 18 h of ambient exposure.

Finally, we note that a series of preliminary experiments with ω-octadecyl and other alkyl isocyanides, performed on Au and Pd substrates identical to the present ones, show no evidence for formation of isocyanate under any of the above conditions.[101] Thus, the propensity for ambient-induced degradation appears much higher for the aromatic-based analogues. This difference could be due to the intrinsic differences in the isocyanide groups in the alkyl and aryl molecules, e.g., polarity of and conjugation effects, or to the higher packing density of the alkyl systems which could slow diffusion of reactive [O] species to the substrate surface. A further understanding of the fundamental mechanisms involved in these surface degradation processes will require extensive experimental work, including single-crystal substrates, in-situ characterization, controlled UHV conditions with dosing by oxygen and other reactants, augmented by in-depth quantum chemical calculations based on multiple metal clusters, as opposed to the preliminary results presented here on metal atom dimers.

Overall, these results illustrate the care that must be taken in the preparation and subsequent exposure of these films in order to obtain and maintain the intrinsic molecular and substrate junction structure. In general, the Au films are much less stable to solvent and oxidative exposure than the Pd ones. Thus the Pd SAMs might be more preferable for applications where either substrate is acceptable. In both cases, the loss of direct headgroup bonding to the metal substrates, which can arise upon storage, can be highly deleterious for such applications as molecular electronic devices where the interface integrity can be a critical parameter in evaluating the intrinsic electrical character of the interface and in the ultimate performance characteristics of the devices.

Acknowledgment. Financial support is acknowledged from the Naval Research Laboratories (J.S., D.A., J.N., R.S.), the Army Research Office (J.S., D.A.), the Defense Advanced Research Project Agency (S.U., D.A.) and the Office of Naval Research (O.C., D.A.). The authors acknowledge Andrew Ichimura for helpful discussions.

Supporting Information Available: Synthesis of the OPE-NC (**1**); density functional quantum chemical calculations of the vibrational modes and intensities of isolated molecule **1** and interactions of molecule **1s** with Au and Pd atoms; IR mode assignments for **1**−Pd SAM; and isotropic optical function spectra for polycrystalline **1**. This material is available free of charge via the Internet at http://pubs.acs.org.

LA051094Z

(101) Stapleton, J.; Harder, P.; Skulason, H.; Bader, M.; Allara, D., to be published elsewhere.